JOURNAL OF CATALYSIS 35, 417–426 (1974)

Photoelectric Work Functions of Ni–Al Alloys: Clean Surfaces and Adsorption of CO

P. E. C. FRANKEN AND V. PONEC

Gorlaeus Laboratoria, Rijksuniversiteit, Leiden, The Netherlands

Received January 2, 1974; revised May 30, 1974

The work function Φ, the emission constant M, and the increase in work function after CO adsorption $\Delta\Phi$ have been measured as a function of the overall composition of well annealed Ni–Al alloy films. The work function of the Ni–Al alloys is not constant within the several miscibility gaps of the Ni–Al phase diagram, and is not lower than the work function of the respective pure metals, as was found with Ni–Cu and Pt–Au alloy films within the miscibility gap. Of all compositions studied only the 25% Ni alloy ($NiAl_3$) distinguishes itself by an increased Φ-value. The higher Φ is explained by the higher atomic density of the $NiAl_3$ compound compared with pure Al and Ni_2Al_3. As with other metal alloy systems, an enrichment of the surface by the component with the lower surface energy (Al) is also found with the ordered Ni–Al alloy system. From $\Delta\Phi$ measurements it appears that up to about 40% Ni the surface of the Ni–Al alloy is composed entirely of Al. The behavior of Φ and $\Delta\Phi$ in the Ni-rich part is explained by the enrichment of the surface by Al. The tendency to form the surface from Al atoms is strengthened by the existence of suitable crystallographic structures. The emission constant does not distinguish any of the intermetallic compounds and resembles that of the Pt–Au and Pd–Ag alloy films.

INTRODUCTION

Several alloy systems have been studied by photoelectric determination of the work function of equilibrated alloy films [Ni–Cu (*1*), Pt–Au (*2*), Pd–Ag (*3*), and others]. Some conclusions of relevance to heterogeneous catalysis emerged from those studies. First, it was shown that the surface of equilibrated alloy films is enriched by the component with the lower surface (sublimation) energy, in accordance with expectation on thermodynamic grounds (Gibbs adsorption). Secondly, it appeared that in two-phase systems such as Ni–Cu and Pt–Au, the surface of alloy films with compositions within the miscibility gap was mainly due to the alloy phase with lower surface energy (i.e., the Cu- or Au-rich phase, respectively). These conclusions were based on self-consistent explanations of the adsorption, catalytic, work function and thermodynamic data.

As a consequence, the work function versus composition plot for the alloys Ni–Cu and Pt–Au differed significantly from that of the completely miscible alloy Pd–Ag. With the former alloys the work function Φ remained constant for all alloy compositions within the miscibility gap. Its value was lower than that of either Ni(Pt) or Cu(Au). The Pd–Ag alloy system, however, revealed a gradual change in Φ, thereby reflecting, most probably, a gradual change in the surface composition. The Φ values for all Pd–Ag alloys remained within the interval between the Φ values of Pd and Ag.

In connection with the photoelectric measurements catalytic experiments were performed with the Ni–Cu, Pt–Au, and Pd–Ag alloys. It was found that the effect

of alloying was in some respects quite different for the three systems. This is not really surprising, as we know that the population of Ni *d*-orbitals does not change by alloying with Cu (see, e.g., the magnetic measurements (*4*), photoemission measurements (*5*), and soft X-ray spectroscopy (*6*), while with Pd the electronic structure changes from the metallic ($4d^{9.6}5s^{0.4}$) to the ($4d^{10}5s^{0}$) structure of a free atom upon alloying with silver (*7*). Further, Ni forms clusters in Ni–Cu alloys (*8*), while Pd is atomically dispersed in its alloys. In both respects Pt–Au is probably more similar to the Ni–Cu system.

We decided to extend the photoelectric work to Ni–Al alloys for the following reasons:

1. The Ni–Al system has a more complicated phase diagram with several well-defined intermetallic compounds and several miscibility gaps. The question arises whether also here minima would be observed in the work function as a function of overall composition.
2. In contrast to the Ni–Cu system the electronic structure of Ni is substantially changed by alloying with Al. The simultaneous increase of the number of "d"-electrons at Ni- and "p"-electrons at Al-atoms (*9*) and the increase of the electronic charge density between Ni and Al alloys (*10*) can be best explained by a covalentlike binding between Ni and Al. This is further supported by the fact that all Al-rich alloys are weakly paramagnetic, as is Al itself. It is an interesting question to ask how these phenomena are reflected in the photoelectric behavior.
3. Due to the ordering in the intermetallic compound structures clustering of Ni is less probable.
4. The photoelectric measurements, particularly when combined with appropriate adsorption studies, can provide some information on the surface composition.

Experimental

(*A*) *UHV Apparatus*

For experimental details of the UHV system with the phototube used and the measuring procedure the reader is referred to a previous paper (*11*). The experiments were carried out in a phototube described therein as tube II. This Pyrex glass tube can be divided into three sections.

(a) The section provided with a heating reflector shield behind which the cathode carrier was kept during preevaporation of the filaments and annealing of the film.
(b) The measuring sections in which an optical Suprasil window is present for transmission of the ultraviolet light.
(c) The evaporation section with two filaments which are divided by a screen in such a way that preparation of pure metal film strips on the cathode support was possible.

Within the phototube there is a cathode carrier consisting of an iron bar clad in Pyrex glass, a baking plate assembly, an oven element and a quartz cathode support with a thermocouple. The cathode carrier can be moved through the tube along W rods by means of magnets.

(*B*) *Alloy Film Preparation*

Aluminum* was evaporated from a multihairpin tungsten filament. In order to obtain a satisfactory pressure during evaporation the Al was first heated above its melting point in 5 Torr H_2. Next, a small part of Al was preevaporated. Thereafter Al was evaporated onto the cathode carrier. During evaporation the phototube was kept at 20°C while the pressure never exceeded 2.10^{-9} Torr.

Nickel was evaporated from a Ni-filament (diam = 0.5 mm*). Otherwise the procedure was similar to the evaporation

*Johnson, Matthey & Co., Ltd., London; spectral pure.

of Al. During evaporation the pressure did not exceed 5.10^{-10} Torr.

The alloy films were prepared by successive evaporation of two films onto each other from the two sources under different angles of evaporation. Janssen and Rieck (*12*) reported a strong Kirkendall effect in this system. Below 600°C diffusion was mainly due to the Al atoms. This situation is very similar to the Ni–Cu and the Pt–Au system, where the equilibration was found to proceed more easily when Ni (or Pt) is evaporated on top of Cu (Au). We therefore evaporated Ni films on top of the Al films. The thickness of the films was 20–50 nm and by means of data given in the paper by Janssen and Rieck the temperature at which such a layer can be brought vertically to equilibrium within a reasonable time was roughly estimated. Finally, the fresh evaporated films were annealed at 618 K for 16 hr in order to bring the alloy to equilibrium. We have also checked that a more prolonged annealing even at still higher temperature did not change further the picture of Φ vs at. % Al curves. X-ray diffraction analysis performed afterwards showed that several different intermetallic compounds were formed. During the annealing at 618 K and during the work function measurements the pressure did not rise above 3.10^{-10} Torr. The results presented below are derived from several measurements on six different alloy films.

(C) *Alloy Film Analysis*

The film prepared in this way revealed a continuously varying composition from 0 to 100 at. % Al. The overall composition of segments, where the work function was measured photoelectrically, was determined for alloys containing >50 at. % Al by neutron activation analysis* and by X-ray diffraction. For the Ni-rich alloys (0–25 at. % Al) X-ray diffraction was found suitable as a method complementary to activation analysis as Végard's law is valid (*13*) here. The composition was derived from the position of the {111} peak. For the 25–50 at. % Al alloys analysis was made as follows. An estimate of the composition of the spots illuminated by the photons in the work function measurements was performed here by X-ray diffraction analysis to check the presence of a given intermetallic compound and by inspecting the color and the position of the spot. The colors were compared to the colors described in ref. (*14*) for well-defined pure compounds.

Special attention was paid to a possible contamination of the films by W. No trace of W was found in clean Al films by neutron activation analysis. When the measurements on clear equilibrated alloy films were finished, carbon monoxide (Air Liquide, Bruxelles; purity > 99.999%) was slowly admitted to the film until the pressure rose to 5.10^{-3} Torr. Subsequently, the photoelectric work function was measured. The work function changes caused by adsorption of CO are denoted below as $\Delta\Phi$.

Results

All photoelectric data can be fitted to the linearized Fowler plot (see Fig. 1). The

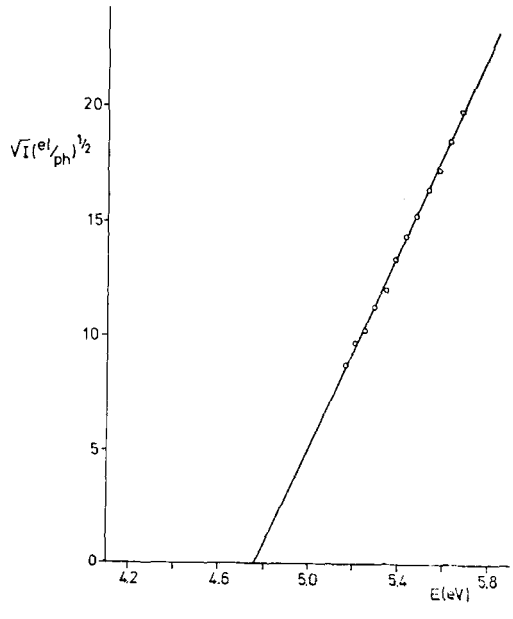

FIG. 1. Fowler plot for a Ni–Al alloy with overall composition of 80 at. % Ni and 20 at. % Al.

* The authors are indebted to Tr. M. de Bruin and his co-workers for the neutron activation analysis of the film.

TABLE 1

VALUES OF THE WORK FUNCTION BEFORE (Φ_{fresh}) AND AFTER ANNEALING ($\Phi_{equilibrated}$), THE EMISSION CONSTANTS (M_{alloy}) DIVIDED BY THE EMISSION CONSTANT OF PURE Al (M_{Al}) AFTER ANNEALING AND THE CHANGE IN Φ ($\Delta\Phi$) AFTER CO ADSORPTION FOR Ni–Al ALLOYS STUDIED

Composition × (at. % Ni)	Φ_{fresh}	$\Phi_{equilibrated}$	M_{alloy}/M_{Al} equilibrated	$\Delta\Phi$ after CO admission
100	5.03	5.03	0.65	1.00
90	4.96	4.90	0.63	0.65
80	4.97	4.74	0.62	0.40
70	4.89	4.665	0.51	0.20
55	—	4.65	0.36	0.25
51	4.46	4.40	0.37	0.20
48	4.38	4.35	0.30	0.04
40	4.33	4.345	0.31	—
26[5]	4.275	4.44	0.34	—
18	4.28	4.395	0.37	—
12	4.27	4.31	0.62	—
0	4.26	4.29	1	—

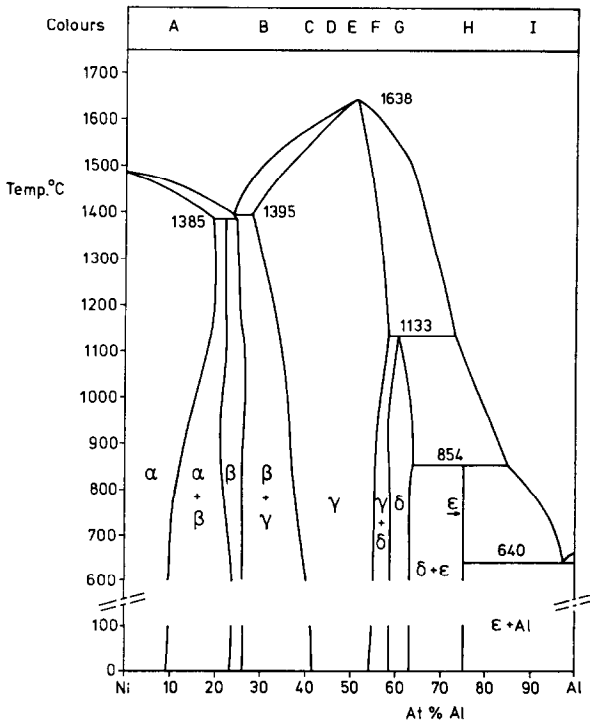

FIG. 2. The Ni–Al phase diagram (Smithells Metal Reference Book, Butterworth, 1967, London) with the changes in color as observed by Bradley *et al.* (*14*) and in this work. A, Ni-like; B, light grey; C, dark grey; D, mauve grey; E, azure blue; F, peacock blue; G, silver; H, pink; I, Al-like.

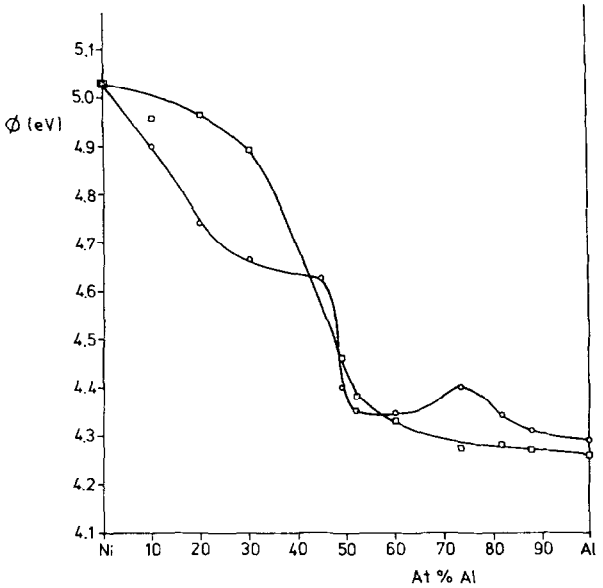

FIG. 3. The work function (Φ) of a freshly sublimed and of an annealed Ni–Al alloy film as a function of the overall composition (at. % Al). □, fresh films; ○, films sintered at 618 K for 16 hr.

phase diagram of the Ni–Al alloy system together with the colors observed by Bradley and Taylor (*14*) and by us are shown in Fig. 2. Relevant values of the work function Φ, the emission constant M and the work function changes $\Delta\Phi$ upon adsorption of CO are compiled in Table 1. Figure 3 shows Φ as a function of overall composition for a freshly evaporated Ni–Al film and for a well sintered film (618 K, 16 hr). Several things can be seen immediately. First, the Φ values of pure Ni

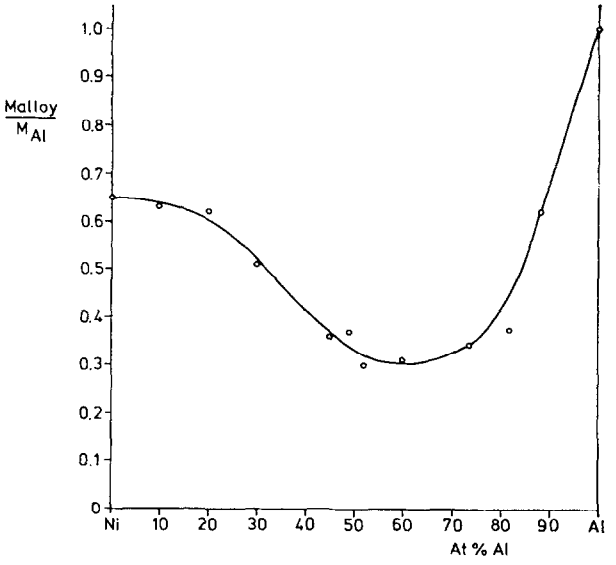

FIG. 4. The emission constant of the alloy (M_{alloy})/the emission constant of pure Al (M_{Al}) of equilibrated Ni–Al alloy films as a function of the overall composition.

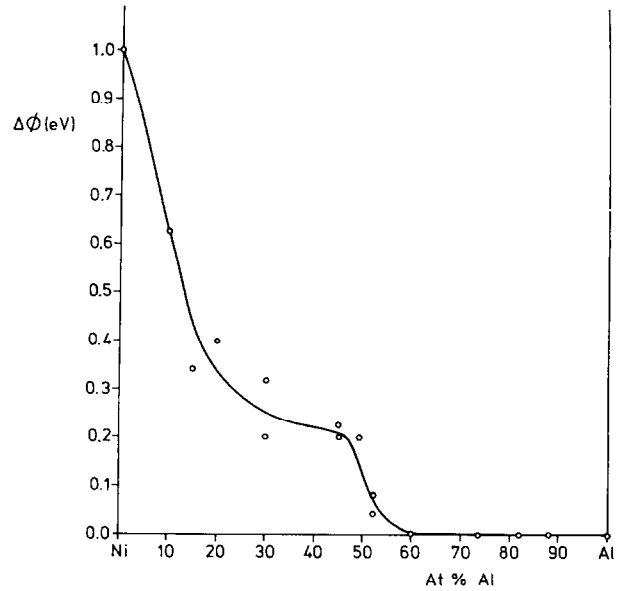

FIG. 5. The change in work function after CO admission to equilibrated Ni–Al alloy films as a function of the overall composition.

and pure Al agree well with the values given in the literature (*15*, *16*). Second, equilibration of the film brings about pronounced changes of Φ. Two points should be noticed, namely the course of Φ for the alloys containing less than 50% Al and the increased Φ for compositions near to that corresponding to the compound $NiAl_3$. Quite remarkable is also the break in Φ values of the equilibrated alloy films around 50 at. % Al. Figure 4 shows the emission constant M as function of the composition of well annealed Ni–Al alloy films. Except for the absence of a maximum the shape of the graph is similar to that observed with Pt–Au and Pd–Ag alloys.

Figure 5 shows the work function changes ΔΦ caused by CO adsorption on Ni–Al alloys. Again the value of ΔΦ for clean Ni of +1 eV agrees well with the values in the literature (*17*). Two points are essential for further discussion. First no measurable change in Φ is observed for all alloys with more than 55 at. % Al. Second, the ΔΦ values for alloys with Al content between 25 and 45% Al form a plateau, quite analogous to the values of Φ the work function of clean surfaces, which show a similar (plateau) constant behavior.

DISCUSSION

Let us first discuss the alloys on the Al-rich side of the phase diagram, i.e., alloys with more than 50 at. % Al. According to the phase diagram there are two phases present within the composition range of 75–100 at. % Al: the Al- and the ε-phase ($NiAl_3$). At an Al-content lower than 75 at. % the Al-phase disappears and the δ-phase (Ni_2Al_3) starts to grow. The ε-phase ($NiAl_3$) is present down to 63 at. % Al and according to the melting points of the respective alloys, and our experience with other two-phase systems, the ε-phase ($NiAl_3$) tends likewise to accumulate at the surface of the alloys with an Al-content between 75 and 63 at. %. This compound, with a very complicated structure, has several densely packed crystallographic planes which might be expected in the surface and which contain only Al. So there is a very wide composition range (100–63 at. % Al) where the top layer is formed by Al-atoms only. That this is true is

shown by the zero value of $\Delta\Phi$ after CO adsorption on all these alloys. According to our data for clean Al and according to Trapnell (*18*) there is no CO adsorption on pure Al.

In the composition range where there are only Al atoms in the surface the work function Φ of the clean surface is not constant but reveals a maximum. This maximum can be explained by the following. Alloys with 75 at. % Al ($NiAl_3$) have a lower volume per alloy atom than the alloys with lower or higher Al content (Al and Ni_2Al_3) (see Table 2). Now several empirical and semiempirical considerations on Φ predict a higher Φ for more densely packed layers of the same metal (*19*).

It therefore seems to be safe to connect the maximum in Φ with the maximum of packing density. The higher Φ-value may be caused by the changes of the surface double layer; at least this seems to be the simplest explanation for the observed phenomenon. If the surface double layer of the clean metal surface is formed by electrons which escape from the metal surface into the vacuum and if each Al atom contributes to this double layer a constant fraction of electrons, an increase of Φ should be expected with increasing density of packing. In this way the results of 100–63 at. % Al alloys can be explained.

Considering the remaining part of the data on the Ni–Al alloys (0–63 at. % Al) there are two aspects which have to be discussed: (I) the reason of the decrease of Φ due to the alloying of Ni with Al; and (II) the shape of Φ vs at. % Al curves. We believe that for the explanation of the first point, the electronic structure of the alloys must be considered, while with the second point we shall turn our attention to the structural (geometrical) aspects of alloying.

I. Al can lower the Φ of the Ni–Al alloy as compared with pure Ni by decreasing the surface dipole, when this is oriented in the expected way with a negative charge to the vacuum. Another possibility is that by alloying Ni with Al the density of electron states (N(E)) as compared to pure Ni changes in such a way that near to the vacuum energy level electron states are created which are localized on Al.

II. The shapes of the Φ vs at. % Al curves show up the following features: a steep *decrease* between 0 and 25 at. % Al; a *plateau* between 25 and 45 at. % and a *steplike decrease* between 45 and 50 at. % Al. This course can be explained as follows.

Ni and Al have very different surface tensions, namely 845 dynes/cm for Al (*20*) and 1756 dynes/cm for Ni (*21*), both at their respective melting points. According to our experience (*1–3*) we expect an enrichment of the surface by Al. Our previous work (*1–3*) has been done on random alloys but, as we shall show below, the enrichment in ordered structures such as Ni–Al compounds can even be stimulated

TABLE 2
THE STRUCTURE AND THE ATOMIC VOLUMES OF Ni–Al INTERMETALLIC COMPOUNDS

Intermetallic compound	Structure	Dimensions unit cell Å	Number of atoms unit cell	Atomic volume Å^3
Ni	fcc	a = 3.52	4	10.91
$Ni_3Al(\beta)$	fcc	a = 3.56	4	11.28
$NiAl(\gamma)$	bcc	a = 2.88	2	12.07
$Ni_2Al_3(\delta)$	trigonal	a = 4.03 c = 4.89	5	15.88
$NiAl_3(\epsilon)$	orthorhombic	a = 6.60 b = 7.35 c = 4.88	16	14.80
Al	fcc	a = 4.07	4	16.89

by the existence of these structures. In other words the surface composition is dictated by the relative stability of the various crystallographic planes. The following considerations are not suggested as a final proof for the described crystallographic surface structures. The considerations have only to show that the crystal structure of alloys makes the observed enrichment of the surface possible and easier.

When Al is added to Ni it dissolves up to 10 at. % Al forming an α-phase. The surface of well equilibrated Ni films is formed by {111} and {100} planes (*22*) and the same holds for the α-phase which has the same fcc structures as Ni. Because of its lower surface energy Al accumulates in this solution near the surface. Increasing the Al content leads to the formation of Ni_3Al, an ordered structure (β-phase). In this concentration region the surface is formed again by {111} and {100} planes; however, the contribution of {100} planes is probably higher because in the Ni_3Al structure the {100} planes contain more Al atoms which contribute less to the total surface energy. This effect can probably easily overcompensate the effect of the lesser density of atoms on {100} planes and higher number of Ni–Al bonds, which have to be broken by forming a {100} plane.

From the foregoing we can understand now the plateau between 25 and 45 at. % Al. The stable {100} plane of Ni_3Al and the most stable {110} plane of NiAl (bcc) (this is the next phase formed when the Al content is increased) have a very similar arrangement of Ni and Al atoms, as can be seen from Fig. 6. So we expect no pronounced changes of Φ in the region where β- and γ-phases (Ni_3Al and NiAl) can coexist (25–42 at. % Al). The enrichment of the surface by the alloying component with the lowest surface energy, as supposed here in ordered structures, has indeed been found by Bouwman (*23*) for Pt_3Sn and PtSn. Around 50 at. % Al very abrupt changes occur in Φ, in the color (*14*), in the fracture (*14*) and in $\Delta\Phi$ upon CO adsorption. This is because the NiAl compound has a high sublimation energy, and thus probably a high surface energy.

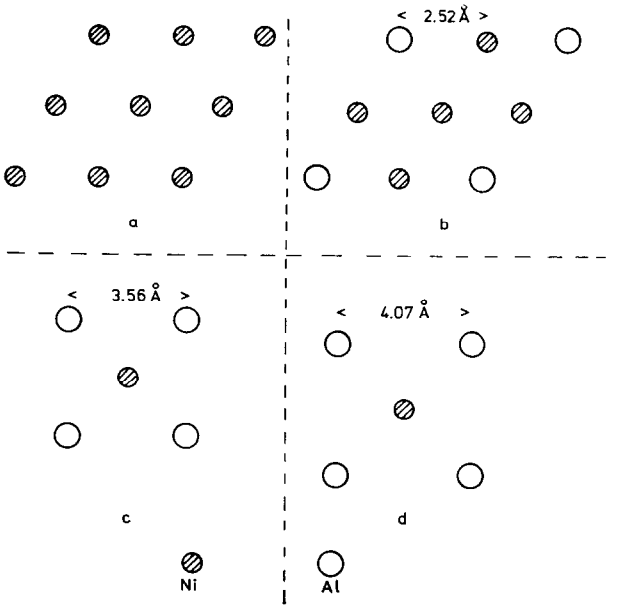

FIG. 6. Crystal surface structures of various Ni–Al compounds: (a) Ni; {111} faces, (b) Ni_3Al; {111} faces, (c) Ni_3Al; {100} faces and (d) NiAl; {110} faces. A successive transformation from (a) to (d) is suggested to explain the course of Φ vs at. % Al in the Ni–Al alloy from 0 up to 50 at. % Al.

Further addition of small amounts of Al leads to the formation at the surface of the structure with a lower sublimation energy, namely, Ni_2Al_3 ($Ni_{1-1/3}Al$). This is actually the same bcc structure as NiAl, only one-third of the Ni atoms is missing. This structure can already have a surface formed by planes with only Al (see Fig. 6; if the central Ni atom is one of the one-third of the total Ni atoms which are missing, the surface contains only Al).

Also the surface of $NiAl_3$ (ϵ-phase) is formed by Al only so that there is no CO adsorption observable on alloys with more than 50 at. % Al. In this way the data on the whole range of compositions are explained.

The emission constant M (reflected by the slope of the linearized Fowler plot) is a very complicated parameter. Some surface effects (e.g., the macroscopic effects on the ratio reflection/absorption of quanta) and volume effects contribute to it. It is remarkable that M does not distinguish any of the several intermetallic compounds. It seems that M depends more strongly on other factors than the crystal structure.

Conclusions

1. In comparison with Ni–Cu and Pt–Au, the Ni–Al system does not show minima in Φ as a function of the overall composition within any of its miscibility gaps.

2. Only the Φ value of $NiAl_3$ distinguishes itself from the surrounding compositions of higher density.

3. As with Ni–Cu, Pt–Au, and Pd–Ag, in NiAl an enrichment of the surface with the metal with the lowest surface energy (Al) occurs.

4. The course of Φ and $\Delta\Phi$ as a function of the overall composition can be rationalized by the following changes in the surface structures with the increasing Al content:

Ni: (111) and (100) planes;
α-phase: enrichment of the surface by Al, (100) planes;
β-phase (Ni_3Al): (100) planes;
γ-phase (NiAl): (110) planes.

5. The emission constant M behaves like M of the well annealed Pt–Au and Pd–Ag alloys and does not distinguish any of the intermetallic compounds.

Acknowledgments

The investigations were supported by the Netherlands Foundation for Chemical Research (S.O.N.) with financial aid from the Netherlands Organization for the Advancement of Pure Research (Z.W.O.). The authors are indebted to Mr. F. C. Kauffeld for skilfully developing and constructing the phototube.

References

1. Sachtler, W. M. H., and Dorgelo, G. J. H., *J. Catal.* **4**, 654 (1965).
2. Bouwman, R., and Sachtler, W. M. H., *J. Catal.* **19**, 127 (1970).
3. Bouwman, R., Lippits, G. J. M., and Sachtler, W. M. H., *J. Catal.* **25**, 350 (1972).
4. Dutta Roy, S. K., and Subrahmanyam, A. V., *Phys. Rev.* **177**, 1133 (1969).
5. Seib, D. H., and Spicer, W. E., *Phys. Rev.* **B2**, 6, 1676 (1970).
6. Wenger, A., Bürri, G., and Steinemann, S., *Phys. Lett.* **34A**, 3, 195 (1971).
7. Stocks, G. M., *Int. J. Quant. Chem.* **5**, 533 (1971); Montgomery, H., Pells, G. P., and Wray, E. M., *Proc. Roy. Soc. Ser. A* **301**, 261 (1967).
8. Hicks, T. J., Rainford, B., Kouvel, J. S., Low, G. G., and Comly, J. B., *Phys. Rev. Lett.* **22**, 531 (1969).
9. Wenger, A., Bürri, G., and Steinemann, S., *Solid State Commun.* **9**, 1125 (1971).
10. Das, B. N., and Azaroff, L. V., *Acta Met.* **13**, 827 (1965).
11. Bouwman, R., and Sachtler, W. M. H., *J. Catal.* **26**, 63 (1972).
12. Janssen, M. M. P., and Rieck, G. D., *Trans. AIME* **239**, 1372 (1967).
13. Bradley, A. J., and Taylor, A., *Phil. Mag.* **S7**, 23, 158, 1049 (1937).
14. Bradley, A. J., and Taylor, A., *Proc. Roy. Soc. Ser. A* **159**, 56 (1937).
15. Wedler, G., Wölfing, C., and Wissmann, P., *Surface Sci.* **24**, 302 (1971).
16. Batt, R. J., *J. Appl. Optics* **9**, 1, 79 (1970).
17. Suhrmann, R., Ober, H., and Wedler, G., *Z. Phys. Chem. NF* **29**, 305 (1961).
18. Trapnell, B. M. W., *Proc. Roy. Soc. Ser. A* **218**, 566 (1953).

19. SACHTLER, W. M. H., *Ber. Bunsenges. Phys. Chem.* **59,** 2, 119 (1955); ALBRECHT, H. E., *Phys. Stat. Sol.* (a) **6,** 135 (1971).
20. NAIDITSCH, E., *Fiz. Metal. Metalloved.* **11,** 883 (1961).
21. SMIRNOVA, O., *Zh. Fis. Chimii* **33,** 771 (1959).
22. STRANSKI, I. N., *Discuss. Faraday Soc.* **5,** 13 (1949).
23. BOUWMAN, R., TONEMAN, L. H., AND HOLSCHER, A. A., *Surface Sci.* **35,** 8 (1973).